Small is Beautiful?
Weakly-Nonlinear Simulations of a Compact WEC for Ocean Monitoring

Harry Bingham and Robert Read
Department of Civil and Mechanical Engineering, Technical University of Denmark
2800 Kgs. Lyngby, Denmark
hbb@dtu.dk

1 INTRODUCTION

Until now, wave-energy developers have focused on designing large machines for utility-scale electricity generation. While many concepts with good capture performance have been devised, significant commercial success has yet to be achieved in this market.

Smaller wave energy converters (WECs) for specialist uses have received less attention. Emerging applications for these machines include powering sensors for ocean monitoring and providing energy for recharging maritime autonomous vehicles. Small reliable floating WECs can provide both the low levels of power required for these applications, and a surface platform for satellite communications. Here, the key idea is to reduce costs and increase human safety by deploying small WECs to perform tasks that would otherwise require a ship.

Developing small WECs for specialist uses provides a fast route to market, thereby creating a viable financial and technical base for the development of larger devices for applications where more power is required. This paper reports early results of time- and frequency-domain simulations of a compact WEC designed for monitoring the ocean environment.

2 DEVICE DESCRIPTION

This paper considers the point-absorber WEC developed by Resen Waves [1]. A cylinder is mounted horizontally on a C-shaped float (see Figure 1(a)). The cylinder's central shaft is rigidly attached to the float, but its outer drum can rotate. A clock spring and gearbox/generator are mounted in parallel between the central shaft and the outer drum, resulting in power absorption as the drum rotates. A mooring line, containing power and communication cables, wraps around the outer drum, descends to an anchor on the seabed, and continues to a sensor unit with battery storage (see Figure 1(b)). A pretension is applied to the mooring line prior to operation. The mechanical power absorbed by the buoy in waves is converted to electrical power that is sent to the battery. The buoy also serves as a communication platform, allowing the sensor unit to transmit data and receive commands via satellite.

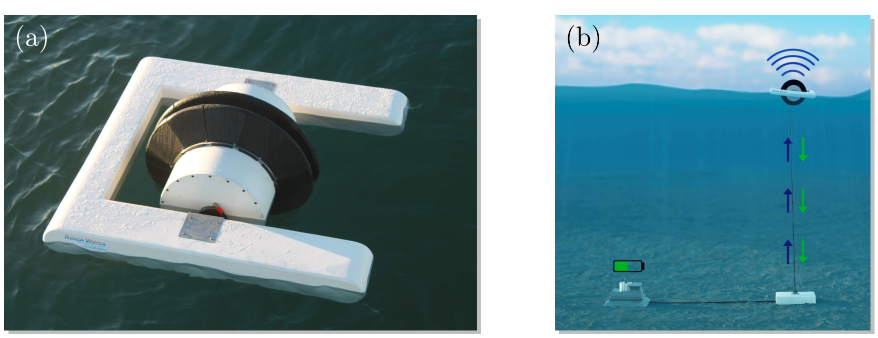

Figure 1: The Resen Waves power buoy: (a) view from above free surface; (b) complete system.

Results are presented for a prototype device which has a rated generator output of 300 W and a peak output of 700 W. The buoy has a length and breadth of 2.75 m and 1.98 m respectively, and the total mass of the float and cylinder is approximately 470 kg.

3 MATHEMATICAL MODELLING

The buoy's equation of motion in the frequency domain is given by,

$$\left[-\omega^2(m_{jk}+a_{jk}+a^*_{jk})+\mathrm{i}\omega(b_{jk}+b^*_{jk})+c_{jk}+c^*_{jk}\right]\frac{\widetilde{\xi}_k}{A}=\frac{\widetilde{F}_{j,\mathrm{d}}}{A}\quad j,k=1,2,\ldots,6. \tag{1}$$

Here, the added mass, a, wave damping coefficient, b, and wave diffraction force per unit wave amplitude, $\widetilde{F}_\mathrm{d}/A$, are calculated using the boundary integral equation method implemented in WAMIT [2]. The hydrostatic stiffness matrix, c, and inertia matrix, m, are constructed from knowledge of the buoy's geometry and mass distribution.

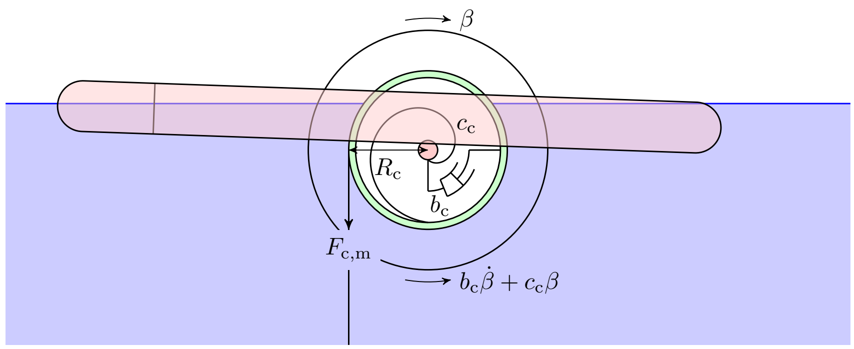

Figure 2: Configuration diagram for frequency-domain model.

In still water, the buoy's weight and buoyancy are balanced by the tension in the mooring cable. As the buoy moves in waves, the PTO system modifies the cable tension. Here, the a^*, b^*, and c^* matrices represent the drum inertia, generator damping, and spring stiffness. This change in the cable tension can be found by applying Newton's second law to the rotation of the drum relative to the float:

$$F_\mathrm{c,m}(t)=-\frac{1}{R_\mathrm{c}}\left[b_\mathrm{c}\dot{\beta}(t)+c_\mathrm{c}\beta(t)\right]. \tag{2}$$

Here, b_c is the equivalent linear damping coefficient of the generator and c_c is the spring stiffness. For small-amplitude motions, the drum's rotation angle, β, and the buoy's response, ξ, are related by

$$\beta=-\frac{\xi_3}{R_\mathrm{c}}-\xi_5. \tag{3}$$

Combining Equations (2) and (3), and re-expressing the result in the frequency domain, leads to

$$\widetilde{F}_\mathrm{c,m}=\frac{1}{R_\mathrm{c}^2}\left[-\omega^2 I_\mathrm{c}\left(\widetilde{\xi}_3+R_\mathrm{c}\widetilde{\xi}_5\right)+\mathrm{i}\omega b_\mathrm{c}\left(\widetilde{\xi}_3+R_\mathrm{c}\widetilde{\xi}_5\right)+c_\mathrm{c}\left(\widetilde{\xi}_3+R_\mathrm{c}\widetilde{\xi}_5\right)\right]. \tag{4}$$

The heave force and pitch moment applied to the buoy through the mooring cable are then given by

$$\widetilde{F}^*_3=-\widetilde{F}_\mathrm{c,m},\quad \widetilde{F}^*_5=-R_\mathrm{c}\widetilde{F}_\mathrm{c,m}. \tag{5}$$

Taken together, Equations (1), (4), and (5) demonstrate that the linear PTO matrices are:

$$a^*_{jk} = \begin{bmatrix} 0 & 0 & 0 & 0 & 0 & 0 \\ 0 & 0 & 0 & 0 & 0 & 0 \\ 0 & 0 & \frac{I_\mathrm{c}}{R_\mathrm{c}^2} & 0 & \frac{I_\mathrm{c}}{R_\mathrm{c}} & 0 \\ 0 & 0 & 0 & 0 & 0 & 0 \\ 0 & 0 & \frac{I_\mathrm{c}}{R_\mathrm{c}} & 0 & I_\mathrm{c} & 0 \\ 0 & 0 & 0 & 0 & 0 & 0 \end{bmatrix}, \quad b^*_{jk} = \begin{bmatrix} 0 & 0 & 0 & 0 & 0 & 0 \\ 0 & 0 & 0 & 0 & 0 & 0 \\ 0 & 0 & \frac{b_\mathrm{c}}{R_\mathrm{c}^2} & 0 & \frac{b_\mathrm{c}}{R_\mathrm{c}} & 0 \\ 0 & 0 & 0 & 0 & 0 & 0 \\ 0 & 0 & \frac{b_\mathrm{c}}{R_\mathrm{c}} & 0 & b_\mathrm{c} & 0 \\ 0 & 0 & 0 & 0 & 0 & 0 \end{bmatrix}, \quad c^*_{jk} = \begin{bmatrix} 0 & 0 & 0 & 0 & 0 & 0 \\ 0 & 0 & 0 & 0 & 0 & 0 \\ 0 & 0 & \frac{c_\mathrm{c}}{R_\mathrm{c}^2} & 0 & \frac{c_\mathrm{c}}{R_\mathrm{c}} & 0 \\ 0 & 0 & 0 & 0 & 0 & 0 \\ 0 & 0 & \frac{c_\mathrm{c}}{R_\mathrm{c}} & 0 & c_\mathrm{c} & 0 \\ 0 & 0 & 0 & 0 & 0 & 0 \end{bmatrix}. \tag{6}$$

In reality, the generator resists the rotation of the cable drum with a constant moment, M_g. An equivalent linear damping coefficient, b_c, is therefore chosen, that dissipates the same average power as the generator. The average mechanical power transferred into the gearbox is given by

$$P = \frac{1}{T}\int_0^T rM_\mathrm{g}\left|\dot{\beta}(t)\right|\,\mathrm{d}t = \frac{2rM_\mathrm{g}\left|\widetilde{\beta}\right|}{T}\int_0^{\frac{T}{2}}\omega\sin(\omega t)\,\mathrm{d}t = \frac{2}{\pi}r\omega M_\mathrm{g}\left|\widetilde{\beta}\right|, \tag{7}$$

where T is the wave period and r is the gearbox ratio. The average power transfer associated with the linear damping coefficient is

$$P = \frac{1}{2}b_\mathrm{c}\omega^2\left|\widetilde{\beta}\right|^2. \tag{8}$$

Equations (7) and (8) can be equated to provide an expression for the equivalent damping coefficient:

$$b_\mathrm{c} = \frac{4rM_\mathrm{g}}{\pi\omega\left|\widetilde{\beta}\right|} = \frac{4rM_\mathrm{g}R_\mathrm{c}}{\pi\omega\left|\widetilde{\xi}_3 + R_\mathrm{c}\widetilde{\xi}_5\right|}. \tag{9}$$

Here, the damping coefficient depends on the wave amplitude and the equation of motion must be solved iteratively. Having calculated the buoy's response, and the mechanical power transfer to the PTO, the electrical power output can be identified from the generator's performance characteristic.

The buoy's equation of motion in the time domain is given by,

$$\left(m_{jk} + a^\infty_{jk}\right)\ddot{\xi}_k(t) + \int_0^t K_{jk}\left(t-\tau\right)\dot{\xi}_k\left(\tau\right)\,\mathrm{d}\tau + c_{jk}\xi_k = F_{j,\mathrm{d}}(t) + F^*_j(t) \quad j,k = 1,2,\ldots,6, \tag{10}$$

where m is the buoy's inertia, a^∞ is the infinite-frequency added mass, c is the hydrostatic stiffness, and F^* is the cable force applied to the buoy. The wave radiation force is the convolution of the radiation impulse response function, K, and the buoy's velocity, $\dot{\xi}(t)$. The wave diffraction force is found by Fourier-transforming the free-surface elevation, multiplying by the frequency response function of the diffraction force, and taking the inverse Fourier transform.

The nonlinear PTO force, F^*, is evaluated at each time step. Taking the drum to be fixed relative to the float, a total cable length, L_c, can be defined to be the sum of: 1) the cable length between the anchor and the tangent to the drum, and 2) the cable length wound onto or let off the drum since starting the simulation. The actual rotation of the drum relative to the float is then

$$\beta = \frac{L_\mathrm{c,e} - L_\mathrm{c}}{R_\mathrm{c}}, \tag{11}$$

where $L_\mathrm{c,e}$ is the length of deployed cable when the buoy is at its initial, equilibrium position. The cable tension generated by the PTO spring and generator is then given by

$$F_\mathrm{c,m} = \frac{c_\mathrm{c}}{R_\mathrm{c}^2}\left(L_\mathrm{c} - L_\mathrm{c,e}\right) \pm \frac{rM_\mathrm{g}}{R_\mathrm{c}}, \tag{12}$$

where the sign of the last term depends on whether the cable is lengthening or shortening. Knowledge of the cable tension and orientation allows calculation of the force vector acting on the buoy. The drum's angular velocity is identified retrospectively using finite-difference methods, The instantaneous mechanical power input to the gearbox is then given by

$$P_{\mathrm{m}} = r M_{\mathrm{g}} \dot{\beta}. \tag{13}$$

The average electrical power output can be computed thereafter. Equation (10) has been solved for regular waves using the DTUMotionSimulator package, which is publicly available [3]. By comparing $F_{\mathrm{c,m}}$ to the cable tension in still water, cable slackening can also be identified.

4 RESULTS FOR REGULAR WAVES

Figure 3 shows how the prototype's response and mechanical power vary with frequency for regular waves with two steepnesses. The points and lines correspond to time- and frequency-domain solutions respectively. The time-domain results are linear except for the PTO system, which is nonlinear. Present work is focused on situations where the mooring cable loses its pretension and goes into slack. Strategies to deal with these occurrences are also being considered.

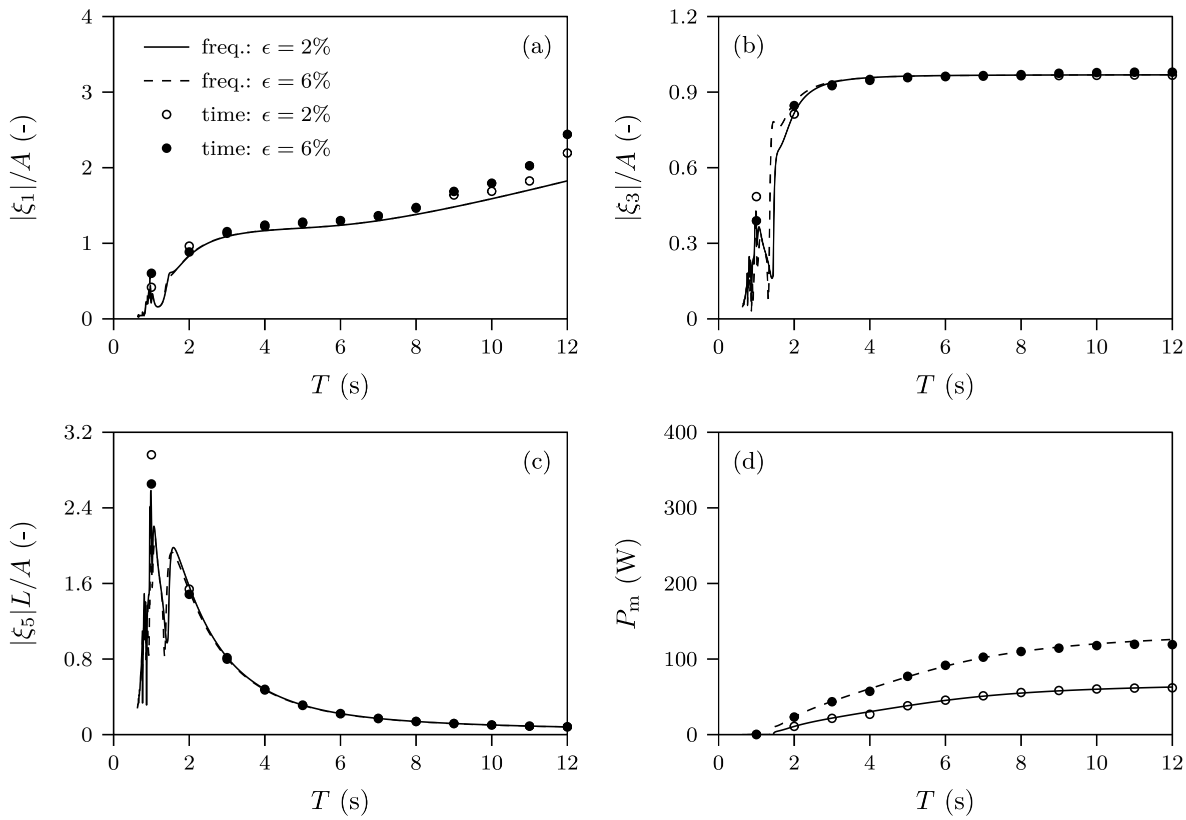

Figure 3: Regular-wave responses and power for prototype device: (a) surge response; (b) heave response; (c) pitch response; (d) mechanical power into gearbox.

[1] Resen Waves. `https://www.resenwaves.com/`, January 2025.

[2] Lee, C.-H., and Newman, J. N. WAMIT User Manual Version 7.0. `http://www.wamit.com/manual.htm`, 2012.

[3] Bingham, H. B. DTUMotionSimulator. `https://gitlab.gbar.dtu.dk/oceanwave3d/DTUMotionSimulator/`, January 2025.